The Journal of Prevention of Alzheimer's Disease 13 (2026) 100479

Contents lists available at ScienceDirect

The Journal of Prevention of Alzheimer's Disease

journal homepage: www.elsevier.com/locate/tjpad

Original Article

Cerebral haemodynamics and white matter hyperintensities: findings using non-invasive brain imaging

Ashwati Vipin [a], James Xiao Yuan Chen [a], Mervin Tee [b], Saima Hilal [b], Yi Jin Leow [a], Simon Konstandin [c], Klaus Eickel [c,e], Matthias Günther [c,d], Jan Petr [f], Henk JMM Mutsaerts [g], Nagaendran Kandiah [a,h,i,*]

[a] Dementia Research Centre (Singapore), 11 Mandalay Road, Lee Kong Chian School of Medicine, Nanyang Technology University, 308232, Singapore
[b] National University of Singapore, Saw Swee Hock School of Public Health, 12 Science Drive 2, #10-01 117549, Singapore
[c] Fraunhofer-Insitute for Digital Medicine MEVIS, Max-von-Laue-Str. 228359 Bremen, Germany
[d] Mediri GmbH, Heidelberg, Germany
[e] Bremerhaven University of Applied Science, An der Karlstadt 8, 27568 Bremerhaven, Germany
[f] Helmholtz-Zentrum Dresden-Rossendorf, Bautzner Landstraβe 400, 01328 Dresden, Germany
[g] Amsterdam University Medical Centre, Department of Radiology and Nuclear Medicine, Van der Boechorststraat 6a, 1081 BT Amsterdam, the Netherlands
[h] Neuroscience and Mental Health Programme, 11 Mandalay Road, Lee Kong Chian School of Medicine, Nanyang Technological University 308232, Singapore
[i] National Healthcare Group, 90 Yishun Central 768828, Singapore

ARTICLE INFO

Keywords:
Cerebral blood flow
Arterial transit time
Blood brain barrier
White matter hyperintensity
Structural equation modelling
Non-invasive brain imaging

ABSTRACT

Background: Utilizing non-invasive neuroimaging for characterization of blood brain barrier (BBB) changes and perfusion deficits underlying small vessel disease pathobiology including white matter hyperintensities (WMH) remains largely unexplored.

Objectives: We examined the underlying haemodynamics of WMH by assessing complex relationships between cerebral blood flow, BBB permeability and WMH burden.

Design, Setting, Participants: Cross-sectional data from study participants belonging to the community-based Biomarker and Cognition Cohort Study, Singapore was obtained.

Measurements: Brain structural and novel non-invasive multi-echo Arterial Spin Labeling data was obtained from 128 participants to derive cerebral blood flow (CBF), arterial transit time (ATT) and BBB time of exchange (T_{ex}).

Results: Neurovascular measures from BBB imaging comprising lower CBF (β=-0.005; p = 0.0139), longer ATT (β=0.644; p = 0.0132) and shorter BBB T_{ex} (β=-0.002; p = 0.0023) were independently associated with higher WMH and higher age-at-visit. Model fit statistics indicated good fit for the structural equation model with a comparative fit index of 0.975 and Standardized Root Mean Square Residual of 0.074. Structural equation modelling revealed CBF (β=0.533; p < 0.001) and ATT (β=-0.254; p = 0.001) as predictors of BBB permeability. Subsequently higher BBB permeability predicted higher WMH burden (β=-0.387; p < 0.001). Additionally, vascular risk factors comprising higher blood pressure and haemoglobinA1C related to lower CBF and shorter BBB T_{ex}.

Conclusions: Our study highlights that CBF and ATT contribute to BBB permeability, which in turn impacts WMH burden. Vascular risk factors also impact neurovascular measures. These findings add to the growing evidence on the potential role of BBB and perfusion deficits underlying small vessel disease burden.

1. Introduction

The global prevalence of dementia is estimated at approximately 50 million individuals, a figure expected to triple by 2050. Notably, up to 40 % of affected individuals show evidence of cerebral small vessel disease (SVD) pathology or substantial vascular burden, underscoring the major role of vascular mechanisms in dementia [1]. Furthermore, amyloid-β and SVD interact through both additive and synergistic

* Correspondence author at. Dementia Research Centre (Singapore) – Lee Kong Chian School of Medicine, Nanyang Technological University, 11 Mandalay Road, Singapore 308232, Singapore.

E-mail address: Nagaendran_Kandiah@ntu.edu.sg (N. Kandiah).

https://doi.org/10.1016/j.tjpad.2026.100479
Received 6 October 2025; Received in revised form 23 November 2025; Accepted 5 January 2026
Available online 19 January 2026

processes, particularly via blood–brain barrier (BBB) disruption, highlighting the complex interplay between vascular and neurodegenerative pathways [2,3]. Therefore, characterization of SVD in community-based cohorts is critical in elucidating early contributors to cognitive decline in at-risk populations, a significant proportion of which are likely to develop vascular cognitive impairment over time [4].

With the growing global burden of SVD, commonly reflected by high white matter hyperintensity (WMH) burden on MRI and strongly linked to cognitive decline, examining SVD-related mechanisms will enable understanding the pathological drivers of dementia [5,6]. Mechanisms underlying WMH formation, progression and related cognitive impairment likely include cortical structure changes leading to axonal loss and demyelination through Wallerian and anterograde degeneration alongside white matter tract disruptions, all of which are closely linked to neurovascular dysfunction [7,8]. Additionally, pathological processes including BBB dysfunction, inflammation and hypoperfusion may also contribute to increased SVD pathology [9,10]. Indeed, increased BBB permeability, representing BBB breakdown, has been demonstrated in vascular cognitive impairment [11]. Specifically, the BBB operates within the neurovascular unit at the juncture between neuronal activity and cerebral blood flow [10,12]. Dysfunction of this neurovascular unit has been linked to not just SVD, but also the amyloid cascade, neuroinflammation and neurodegeneration, illustrating its role in dementia onset and progression [9,12,13] Importantly, prior findings indicate that BBB dysfunction may initiate WMH formation, especially accompanying SVD-related perfusion deficits [14,15]. Thus, reliable neuroimaging characterization of BBB and perfusion deficits in early cognitive impairment, particularly those underlying WMH, is crucial for early detection, biomarker development and intervention.

In this regard, dynamic contrast-enhanced-magnetic resonance imaging has illustrated hippocampal BBB deficits in pre-dementia stages using Gadolinium-based contrast agents [11,16]. However, contrast agents have large molecular sizes, enabling detection of major BBB disruptions only [17]. Thus, non-invasive brain imaging to measure SVD-related subtle BBB dysfunction is needed [18]. A multi-echo Hadamard-encoded multi-post-labeling-delay pseudocontinuous-arterial spin labelling (ME-ASL) under DEveloping Blood-Brain barrier arterial spin labeling as a non-Invasive Early biomarker (DEBBIE) protocol has emerged as a promising technique for detecting early BBB changes. This ME-ASL sequence uses the exchange time of small molecule labelled water to move across the BBB (T_{ex}) as a sensitive proxy measure of BBB integrity and can detect age-related BBB changes in humans with excellent test-retest reliability [19–22]. However, its use in SVD remains largely unexplored.

Taking into consideration the above gaps, our aim was to examine the haemodynamics underlying WMH using non-invasive BBB imaging in non-demented subjects from a community-based cohort. We sought to decipher potential complex relationships between neurovascular measures involving blood flow, BBB permeability and WMH burden. We hypothesized that neurovascular changes and BBB permeability would be significant contributors to increased WMH burden.

2. Methods

2.1. Participants

Participants were recruited as part of a community-based research cohort from the Dementia Research Centre (Singapore). Inclusion criteria comprised the presence of any cognitive concern among individuals from the community aged between 30 and 95, inclusive of limits. Key exclusion criteria included illiteracy wherein participants are unable to read or write, diagnosis of major psychotic, psychiatric, neurological disorders and serious systemic disease [23]. Participants with cross-sectional ME-ASL neuroimaging and blood-based assessments and blood pressure measurements (mmHg) only were included in this study.

2.2. Blood-based assessments

Participants underwent a blood draw and samples were sent to Innoquest labs for deriving levels of Hemoglobin A1C (HbA1c) and total cholesterol.

2.3. Neuroimaging acquisition

All participants underwent whole-brain MRI using a 3T Siemens Prisma Fit scanner (Siemens Healthineers, Erlangen, Germany). The T1-weighted accelerated magnetization-prepared rapid gradient-echo sequence comprised the following parameters: repetition time (TR) = 2000 ms, echo time (TE) = 2.26 ms, inversion time (TI) = 800 ms, flip angle = 8°, matrix size = 256 × 256 × 176 and voxel size = 1.0 × 1.0 × 1.0 mm3. The Fluid Attenuated Inversion Recovery sequence comprised of the following parameters: 192 continuous sagittal slices, TR/TE/TI = 7000/394/2100 ms, flip angle of 120°, FOV of 256 × 256mm2, matrix of 320 × 320, isotropic voxel size of 0.8 × 0.8 × 1.6 mm3, and bandwidth of 650 Hz/pixel. Additionally, participants also underwent two ME-ASL scans using multi-TE pCASL with a segmented 3D-GRASE readout with different bolus durations acquired according to the DEBBIE protocol [21,24]. The first protocol was acquired using two repetitions (post labelling delay(PLD)=0.6 and 0.8 ms) of a Hadamard-8 matrix with sub-bolus duration=400 ms resulting in 14 PLDs[600, 800,… 3200], two averages, repetition time(TR) of 4000 ms, and a single-echo (echo time(TE)=11.6 ms) readout optimised for ATT and CBF quantification. The second scan was acquired using a Hadamard-4 matrix with sub-bolus duration=1000 ms, three post-labelling delays [500,1500, 2500]ms, TR of 4500 ms and a multi-echo (TE=[11.6:34.9:174.6]ms) readout optimised for BBB Tex quantification [25]. The field-of-view was set to be 320 × 160 × 160 mm^3 with isotropic nominal resolution of 5 mm. Two background suppression pulses timed to suppress T1 values of 700 and 1400 ms were applied. A separate M0 scan without labeling train and background suppression was performed with a TI of 1700 ms.

All scanned images were reviewed during and post-acquisition, and participants with severe motion artifacts and overt pathological findings were excluded from analysis.

2.4. Neuroimage pre-processing

White matter hyperintensity volumes were derived using the lesion segmentation toolbox in SPM12, by extracting binary WMH lesion belief maps. The lesion prediction algorithm toolbox algorithm co-registers the T2 FLAIR image to T1 image and subsequently segments T1 images into grey matter, white matter, and cerebrospinal fluid tissue maps. Binary lesion maps are created by thresholding the grey matter, white matter, and cerebrospinal fluid tissue maps as well as a spatial covariate that considers voxel specific changes in lesion probability. Parameters of this model fit were used to segment lesions in new images through estimates for the lesion probability for each voxel [26]. Total WMH lesion volume for each participant was obtained using the "extract values of interest" option in the lesion segmentation toolbox.

Total WMH lesion volumes were log transformed in all statistical analyses. In subsequent sections, WMH load will refer to log-transformed WMH.

2.5. Explore ASL pipeline

Cerebral blood flow (CBF), T_{ex} and arterial transit time (ATT) quantification was performed using ExploreASL version v1.11(https://exploreasl.github.io/Documentation/1.11.0/) [24,25]. ASL quantification was performed with FSL version 6.0.7.11(https://fsl.fmrib.ox.ac.uk/) with a dedicated ME-ASL quantification module [25]. ExploreASL has integrated several toolboxes together as a single pipeline to process ASL images automatically. Structural segmentation was performed using CAT12 (https://neuro-jena.github.io) automatic pipeline. A 3-compartment model was used with an arterial compartment, capillary intravascular compartment, and extravascular compartment. Four parameters are fitted within this model: ATT, CBF, time parameter T_{ex} describing the exchange across the BBB, and intra-voxel transit time parameter describing the time delay the labelled blood needs to reach the capillary compartment from the arterial compartment. Hadamard 4 and Hadamard 8 data were concatenated, and all four parameters were fitted jointly on a voxel-wise basis [24,25]. Quantification was done voxel-wise on data concatenated from both Hadamard 8 and Hadamard 4 data. This MATLAB-based software was used with MATLAB (MathWorks, MA, USA) version 9.13 (R2022b) (https://www.mathworks.com/products/matlab.html). The threshold of grey matter region subsampling to the ASL voxel-size was set to 70 % and used as a grey matter region of interest.

2.6. Statistical analyses

We first examined bivariate associations between neurovascular variables of CBF, ATT and BBB T_{ex} with age-at-visit and log-transformed WMH volume using linear regressions. Age-at-visit, sex and education years were covariates.

We used structural equation modelling using the lavaan package to assess the contribution of neurovascular variables grey matter CBF and ATT to BBB T_{ex} and subsequent BBB T_{ex} contribution to WMH burden. This enabled simultaneous estimation of multiple relationships and interrelationships among various variables, considering the interdependencies among them. This model was also used to examine how much variance in WMH is explained by CBF, ATT and BBB T_{ex}.

The CBF latent construct comprised CBF adjusted by noise, random noise and squared non-linear transformation to account for non-linear relationships between CBF and WMH as well as measurement error. The ATT latent construct comprised ATT adjusted by noise, random noise and log transformation to handle skewness as well as measurement error. These latent variables were created to capture both linear and non-linear effects appropriately. The covariance between ATT and CBF variables was considered in the model (i.e. double-headed arrows) to correct for an overestimation of the relationship between independent and dependent variables.

Fit indices comprising the comparative fit index, root mean square error of approximation, and standardized root mean square residual were examined to assess the fit of the model. We considered a comparative fit index>0.90 and a standardized root mean square residual<0.08 to be acceptable model fit indexes as per Hu and Bentler's Two-Index Presentation Strategy [27]. Structural equation modelling was applied to fit the structural model of regression relationships between the variables CBF latent variable, ATT latent variable, T_{ex} measured variable and log-transformed WMH volumes simultaneously using The "semTools" package (version 0.5–6).

As an exploratory analysis, we examined the association between neurovascular variables CBF and BBB T_{ex} and vascular risk factor measures including systolic blood pressure, diastolic blood pressure, HbA1c and total cholesterol. Linear regression analyses was conducted and ATT, age-at-visit, sex and education years were added as covariates.

All analyses were performed using R version 4.1.1 (R Core Team, 2021). A 2-sided $p < 0.05$ was considered statistically significant.

3. Results

A total of 128 subjects with a mean age of 57.6 (±11.3) years with non-invasive BBB imaging were included in the examination of the haemodynamics underlying WMH (Table 1). Further participant characteristics of the sample with BBB imaging are summarised in Table 1.

Table 1
Demographics and Clinical Characteristics of BBB Imaging Subset.

	Characteristics (n = 128)
Age at visit (years) †	57.6 ± 11.3
Sex, female ⸸	84 (65.6 %)
Education years †	15.2 ± 3.6
Visual Cognitive Assessment Test †	26.9 ± 3.1
Montreal Cognitive Assessment †	26.4 ± 2.5
Diastolic blood pressure (mmHg) †	77.1 ± 11.8
Systolic blood pressure (mmHg) †	124.1 ± 17.1
Total cholesterol (mmol/L) †	5.4 ± 1.2
HbA1c (%) †	5.8 ± 0.5

Note. † = mean ± Standard Deviation, ⸸ = Frequency (percentages).

3.1. Association of grey matter blood perfusion, arterial transit time and blood brain barrier permeability with age-at-visit

Linear regression analyses illustrated significant relationships between CBF, ATT, BBB T_{ex} and age-at-visit after controlling for sex and years of education. Specifically, older participants demonstrated lower CBF (β=−0.37;p = 0.0022; Table 2), longer ATT (β=0.006;p < 0.001; Table 2) and shorter BBB T_{ex} (increased permeability) (β=−0.99;p = 0.012; Table 2).

3.2. Association of grey matter blood perfusion, arterial transit time and blood brain barrier permeability with white matter hyperintensities

Linear regression analyses illustrated significant relationships between CBF, ATT, BBB T_{ex} and log WMH after controlling for age-at-visit, sex and years of education. Specifically, lower CBF related to higher WMH burden (β=−0.005;p = 0.0139;Fig. 1A; Table 3), longer ATT related to higher WMH burden (β=0.644;p = 0.0132;Fig. 1B; Table 3) and shorter BBB T_{ex} (increased permeability) related to higher WMH burden (β=−0.002;p = 0.0023;Fig. 1C; Table 3). Additionally, there was no association between WMH burden and ME-ASL head motion.

3.3. Structural equation modelling between CBF, ATT, BBB permeability and WMH

Structural equation modelling revealed important relationships between CBF and ATT on BBB T_{ex}. Because of the large sample size relative to model parameters, significant $\chi 2$ test was obtained (p = 0.001). Fig. 2 illustrates the structural model and the standardized estimates. Model fit statistics indicated good fit for the structural equation model with a comparative fit index of 0.975 and Standardized Root Mean Square Residual of 0.074.

Specific to the structural equation model, the latent variables for CBF and ATT were measured effectively by their indicators. A significant negative covariance between the latent variables indicated an inverse relationship between perfusion and ATT as illustrated by the two-way arrow (standardized covariance ρ=−0.628,p < 0.001;Fig. 2). Importantly, the regression paths showed significant relationships between CBF and BBB T_{ex} (standardized β=0.497,p < 0.001), ATT and BBB T_{ex} (standardized β=−0.291,p = 0.001) and eventually BBB T_{ex} with WMH (standardized β=−0.387,p < 0.001) as illustrated in Fig. 2. The R^2 values indicated that 50.6 % variance in BBB T_{ex} was explained by latent variables of ATT and CBF. This suggested that the combination of these

Table 2
Association between grey matter blood perfusion, arterial transit time and blood brain barrier permeability with age-at-visit.

	Beta	P value	CI
Cerebral Blood Flow	−0.37	0.0022	−0.630, −0.146
Arterial Transit Time	0.006	<0.001	0.0049, 0.009
Time of Exchange	−0.99	0.012	−1.786, −0.225

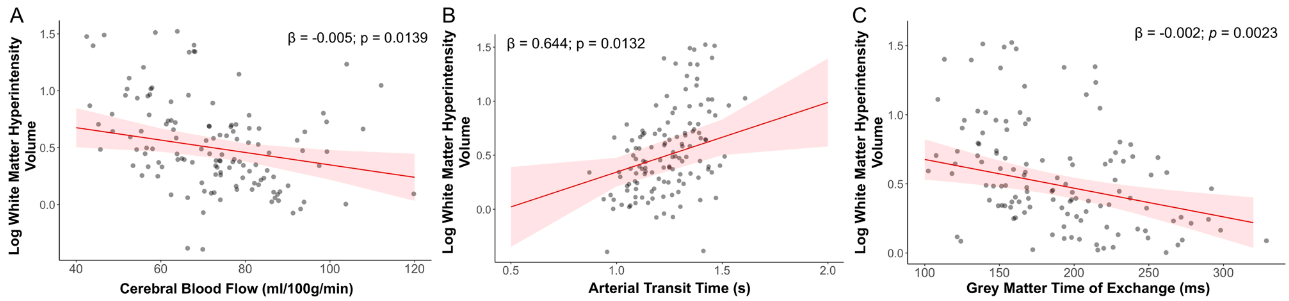

Fig. 1. Cerebral blood flow, arterial transit time and blood brain barrier permeability independently influence white matter hyperintensity burden. A) Lower cerebral blood perfusion was associated with higher white matter hyperintensity burden. B) Prolonged arterial transit time was associated with higher white matter hyperintensity burden. C) Shorter time of exchange of water across the blood brain barrier was associated with higher white matter hyperintensity burden.

Table 3
Association between grey matter blood perfusion, arterial transit time and blood brain barrier permeability with white matter hyperintensities.

	Beta	P value	CI
Cerebral Blood Flow	−0.005	0.0139	−0.009, −0.0011
Arterial Transit Time	0.644	0.0132	0.137, 1.152
Time of Exchange	−0.002	0.0023	−0.003, −0.0007

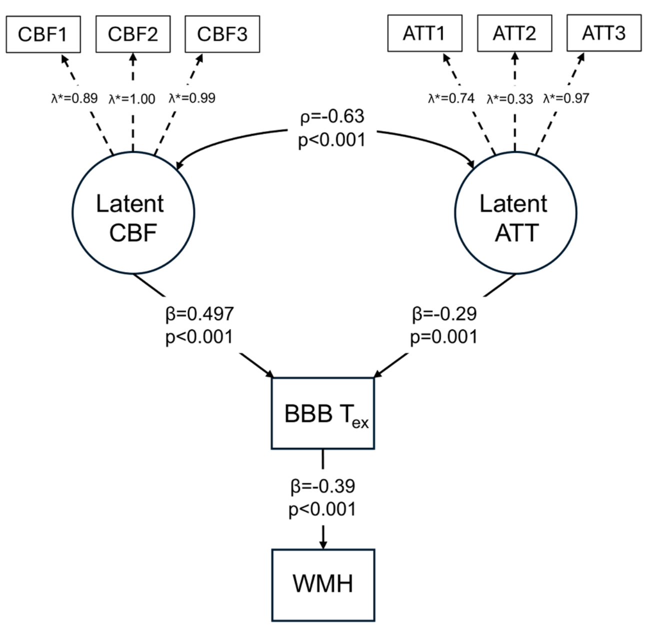

Fig. 2. Path diagram of structural equation model for white matter hyperintensity burden. Reduced cerebral blood flow and prolonged arterial transit time were significant contributors of blood brain barrier dysfunction as indicated by shorter blood brain barrier time of exchange. This was in turn associated with higher white matter hyperintensity burden. Circles represent latent variables and rectangles represent observed variables. Standardized beta (β) coefficients are shown on each unidirectional solid path/arrow and represent the strength and direction of the regression. The double-sided solid arrow with standardized rho (ρ) represents the strength of covariance between latent variables. Unidirectional dashed arrows with standardized lambda* (λ*) represent the factor loadings of each indicator CBF1, CBF2, CBF3 and ATT1, ATT2, ATT3 on their respective latent variable Latent CBF and Latent ATT and indicates how strongly these indicators reflect the latent construct. Abbreviations: CBF, cerebral blood flow; ATT, arterial transit time; BBB T_{ex}, blood brain barrier time of exchange; WMH, white matter hyperintensity.

latent variables for ATT and CBF explained moderate variability in BBB T_{ex}. Additionally, 15 % of variance in WMH was in turn explained by BBB T_{ex}. This indicated the contribution of other factors in addition to those in this model to the variability in WMH. Notably, these associations remained significant when using partial volume corrected values of CBF, ATT and T_{ex}.

3.4. Impact of vascular risk factors on neurovascular measures of cerebral blood perfusion and blood brain barrier permeability

Linear regression analyses examined whether chronic vascular risk factors including measures of HbA1c, total cholesterol, systolic and diastolic blood pressure influenced CBF and BBB T_{ex}. In addition to age-at-visit, sex and years of education, ATT was also controlled for as it has been shown to be associated with a compromised hemodynamic state. Here, lower BBB T_{ex} was associated with higher HbA1c levels ($\beta=-16.79; p = 0.0246$; Table 4). Lower BBB T_{ex} was marginally associated with higher systolic blood pressure ($\beta=-0.417; p = 0.0626$; Table 4). BBB T_{ex} did not relate to diastolic blood pressure and total cholesterol. Lower CBF was associated higher diastolic blood pressure ($\beta=-0.215; p = 0.0205$; Table 4), higher systolic blood pressure ($\beta=-0.147; p = 0.032$; Table 4) and higher HbA1c levels ($\beta=-4.55; p = 0.05$; Table 4). No associations were observed between CBF and total cholesterol.

4. Discussion

In a community-based cohort of non-demented adults, we examined potential hypothesized relationships between neurovascular measures of CBF and ATT, BBB permeability and WMH (Fig. 3). Linear regression analyses illustrated significant associations between lower CBF, longer ATT and shorter BBB T_{ex} (higher BBB permeability) with higher age-at-visit and cerebral WMH burden. Structural equation modelling examined links between CBF and ATT on BBB T_{ex} and subsequently between BBB T_{ex} and WMH. Here, CBF and ATT deficits were demonstrated to be significant contributors to longer BBB T_{ex} which in turn associated with higher WMH burden. In further analyses, higher systolic and diastolic blood pressure and HbA1c levels, but not total cholesterol, were

Table 4
Impact of vascular risk factors on neurovascular measures of cerebral blood perfusion and blood brain barrier permeability.

HbA1c	Beta	P value	CI
Cerebral Blood Flow	−4.55	0.05	−9.135, 0.016
Time of Exchange	−16.79	0.0246	−31.406, −2.191
Systolic blood pressure			
Cerebral Blood Flow	−0.147	0.032	−0.281, −0.012
Time of Exchange	−0.417	0.062	−0.845, 0.022
Diastolic blood pressure			
Cerebral Blood Flow	−0.215	0.0205	−0.396, −0.033
Time of Exchange	−0.375	0.213	−0.967, 0.217
Total Cholesterol			
Cerebral Blood Flow	1.095	0.233	−0.713, 2.904
Time of Exchange	1.393	0.638	−4.447, 7.23

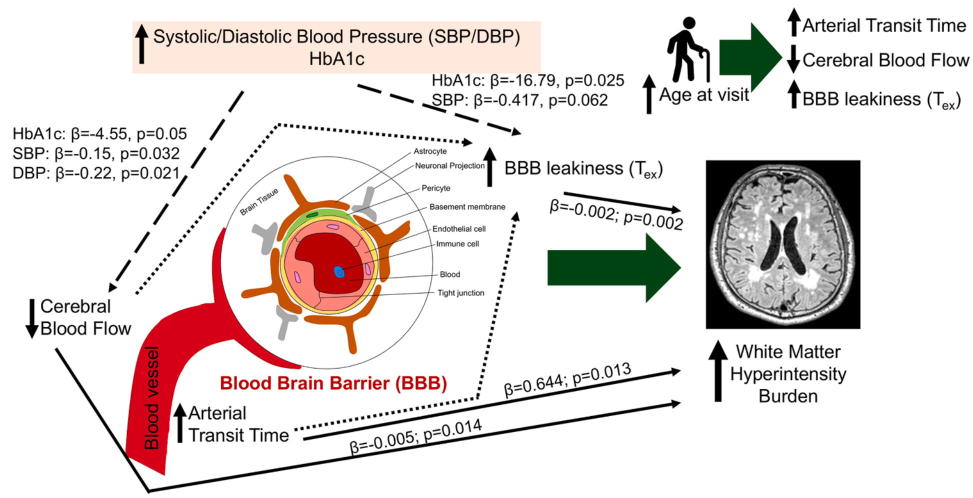

Fig. 3. Overview diagram illustrating links between hemodynamic measures, age, vascular risk factors and white matter hyperintensity burden.

associated with lower CBF and longer BBB T_{ex}.

Prior studies have illustrated links between CBF and ATT and SVD burden [15,28]. Specifically, lower CBF and longer ATT consistently relate to higher WMH burden [28,29]. This is in line with our linear regression analysis demonstrating significant links between lower CBF and longer ATT with higher WMH burden. Shorter BBB T_{ex}, reflective of increased BBB leakiness, was also related to higher WMH burden. We thus reiterate the interplay of neurovascular factors and their possible role in the pathogenesis of WMH.

To build on these linear relationships, we utilised structural equation modelling to enable simultaneous examination inter-relationships among neurovascular variables CBF, ATT and BBB T_{ex} and their impact on WMH burden. Due to our sample size, we opted for a simple model to prevent overfitting. We observed that, expectedly, increases in ATT linked to CBF deficits. Moreover, longer ATT and lower CBF related to increased BBB permeability as determined by shorter BBB T_{ex}. Importantly, significant variance in BBB T_{ex} i.e. 50.6 % was explained by CBF and ATT, thus indicating their importance. These results are in line with evidence illustrating the role of chronic cerebral hypoperfusion in exacerbating BBB dysfunction including endothelial impairment and neurovascular uncoupling in aging [15]. As ATT measures the arrival time of labelled blood water, it has been shown to be sensitive to a compromised hemodynamic state [30]. However, the relationship between ATT and BBB permeability remains largely unexplored. In this regard, our novel results demonstrate the significant association between prolonged ATT and increased BBB permeability. Future studies examining regional ATT with regional BBB permeability will shed light on specific effects on hemodynamic vulnerability.

Moreover, BBB dysfunction through shorter T_{ex} was shown to be significantly associated with higher WMH burden in our study. This is in line with previous rodent studies suggesting that BBB damage may be an upstream process for WMH formation, especially in the context of chronic cerebral hypoperfusion [14,15]. Additionally, cortical structure changes themselves can lead to axonal loss and demyelination due to Wallerian degeneration. Furthermore, WMH may reflect microvascular damage, hypoperfusion and ischaemia which may also underlie BBB dysfunction in overlapping regions [7,31]. Permeability changes in grey matter BBB may also tie closely with WMH since they are vulnerable to the same risk factors, inflammation and vascular aging. Thus, our findings provide important evidence for the proliferation of WMH through increased BBB permeability which is in turn impacted by neurovascular impairment involving hypoperfusion and longer ATT. These findings can have implications on drug targets for WMH and dementia that can specifically improve BBB permeability or cerebral blood perfusion. Additionally, the role of inflammation has also been explored as a possible mechanism underlying BBB dysfunction impact on WMH build up. Such mechanisms likely involve the activation of pro-inflammatory cytokines which set in motion an aggravated feedback loop of WMH build up and BBB disruption [32]. While our model did not examine inflammatory mechanisms underlying BBB damage and WMH, these relationships will need to be studied in detail in future longitudinal studies.

While CBF and ATT explained moderate variability in BBB T_{ex}, 15 % of the variance in WMH was in turn explained by BBB T_{ex}. While BBB dysfunction has been shown to contribute to WMH presence, our results reflect that significant variability in WMH remained unexplained by the model, indicating involvement of other mechanisms including neuroinflammation and neurodegenerative pathology [33]. Additionally, cardiovascular risk factors including hypertension, body mass index, diabetes and hyperlipidaemia have also been shown to explain significant variance in WMH [34]. Notably, our findings are the first to show the potential impact on BBB T_{ex} using non-invasive BBB imaging in a cohort of community-dwelling adults.

Our findings of age-related decline in neurovascular measures of CBF, ATT and T_{ex} are supported by recent studies using the same ME-ASL technique [20]. Exploratory linear regression analyses also examined the association between vascular risk factors of blood pressure, total cholesterol and HbA1c levels on CBF and BBB T_{ex}. We demonstrate that systolic and diastolic blood pressure and HbA1c levels were closely associated with lower CBF and longer BBB T_{ex}. Notably, we controlled for ATT in these analyses since it is closely associated with CBF [28]. Vascular risk factors had a significant impact on lower CBF as well as shorter BBB T_{ex} reflective of both perfusion deficits and increased BBB permeability, respectively. Our findings are also in line with prior studies that have established links between high blood pressure and BBB breakdown through derogatory effects on BBB endothelial cells and pericytes [35]. Such damage may lead to a reduction in CBF and white matter damage [35,36]. Additionally, individuals with type II diabetes demonstrate increased BBB permeability using contrast-based BBB imaging [37]. Animal studies indicate a causal link between diabetes and BBB dysfunction [38]. Related to this, our findings are the first to illustrate such associations in humans using non-invasive BBB imaging. Disruption of cerebrovascular autoregulation related to type II diabetes has been linked to altered CBF. Specifically, regional CBF reduction has been shown to be linked to HbA1c [39]. Our findings align with large population-based cohort studies showing that vascular risk factors contribute differentially to WMH burden. Hypertension and diabetes are consistently associated with greater WMH volume, whereas hypercholesterolemia does not appear to exert a similar effect [40,41]. These observations suggest that WMH pathology may be particularly vulnerable to the effects of elevated blood pressure and impaired glucose metabolism, but not necessarily to elevated total cholesterol levels [41]. The mechanistic pathways linking these risk factors to WMH likely involve chronic BBB dysfunction, arteriosclerosis, and cerebral hypoperfusion, processes also demonstrated in our findings [41–43]. Supporting this vascular perspective, transcranial Doppler studies reveal mixed, dose-dependent associations between low-density lipoprotein levels and intracranial blood flow velocity, underscoring the complex role of cholesterol in cerebrovascular regulation [44]. Thus, stringent blood pressure and diabetes control may comprise first-line targets to improve CBF and BBB function which can in turn reduce WMH. Our findings add to the growing body of literature illustrating important links between vascular risk factors, BBB dysfunction and CBF. These associations will need to be examined further to elucidate temporal relationships.

A novel non-invasive BBB ASL technique which has shown promise in the measurement of BBB changes was utilised in our study [20]. Significant associations between BBB T_{ex} with age have also been observed using BBB ASL such that older participants showed increases in BBB permeability through shorter T_{ex}, lower CBF and prolonged ATT [20]. Through our findings of intricate relationships between CBF, ATT, BBB T_{ex} and WMH, we provide further promising evidence on the robust use of non-invasive BBB imaging in understanding disease mechanisms. Further strengths of our study include the use of a non-demented community cohort to elucidate early haemodynamic changes which can help guide early therapeutic interventions for SVD and related dementia.

However, our study has some limitations. We had a relatively small sample size and utilised a novel BBB ME-ASL technique which may impact the generalisability of our results. Additionally, the cross-sectional design limited our ability to infer causality and temporality. However, we plan to address these limitations with future cross-sectional and longitudinal data. Furthermore, our study did not examine other SVD markers such as lacunar infarcts and cerebral microbleeds, which will be explored in future research. Lastly, as our cohort was community-based, it may include fewer individuals with substantial disease pathology.

In conclusion our study elucidates the possible underlying haemodynamic mechanisms contributing to WMH. Utilising a novel and robust non-invasive BBB ME-ASL imaging technique, our findings indicate the important role of CBF and ATT on BBB permeability, which in turn impacts WMH burden. Upstream vascular risk factors, including high blood pressure and HbA1c levels, influence CBF and BBB T_{ex} which in turn impact WMH as illustrated by our structural equation modelling. These findings add to the growing body of evidence highlighting the importance of managing vascular risk factors to improve cerebral haemodynamics and eventually reduce WMH.

Abbreviations

ASL – arterial spin labelling
ATT – arterial transit time
BBB – blood brain barrier
CBF – cerebral blood flow
DEBBIE – DEveloping Blood-Brain barrier arterial spin labeling as a non-Invasive Early biomarker
HbA1c – haemoglobinA1C
ME-ASL – multi-echo Hadamard-encoded multi-post-labeling-delay pseudocontinuous arterial spin labelling
PLD – Post-labelling delay
SVD – small vessel disease
T_{ex} – exchange time of labelled water across the blood brain barrier
WMH – white matter hyperintensity

Funding sources

This study received funding support from the Strategic Academic Initiative grant (SP1CLNT900-NTU-A630-PJ-03INP001400A630) from the Lee Kong Chian School of Medicine, Nanyang Technological University, Singapore, National Medical Research Council, Singapore under its Clinician Scientist Award (MOH-CSAINV18nov-0007), Ministry of Education Start-up Grant, Ministry of Education Academic Research Fund Tier 1 (RT02/21), Ministry of Education Science of Learning grant (MOESOL2022–0002) and Strategic Academic Initiative LEARN grant (03INP001737A630) from the Lee Kong Chian School of Medicine, Nanyang Technological University, Singapore.

Data availability

Anonymised data will be made available upon reasonable request.

Consent statement

The study was approved by the Nanyang Technological University Institutional Review Board (Reference 2021–1036). All participants provided informed consent in accordance with the Declaration of Helsinki and local clinical research regulations.

CRediT authorship contribution statement

Ashwati Vipin: Writing – review & editing, Writing – original draft, Visualization, Project administration, Methodology, Investigation, Funding acquisition, Formal analysis, Data curation, Conceptualization. **James Xiao Yuan Chen:** Methodology, Formal analysis, Data curation. **Mervin Tee:** Writing – review & editing, Methodology, Data curation. **Saima Hilal:** Writing – review & editing, Methodology, Investigation, Data curation. **Yi Jin Leow:** Writing – review & editing, Project administration. **Simon Konstandin:** Writing – review & editing, Methodology, Data curation. **Klaus Eickel:** Writing – review & editing, Methodology, Conceptualization. **Matthias Günther:** Writing – review & editing, Methodology, Conceptualization. **Jan Petr:** Writing – original draft, Software, Methodology. **Henk JMM Mutsaerts:** Writing – original draft, Software, Methodology, Investigation. **Nagaendran Kandiah:** Writing – original draft, Supervision, Resources, Project administration, Methodology, Investigation, Funding acquisition, Formal analysis, Conceptualization.

Declaration of competing interest

The authors declare that they have no known competing financial interests or personal relationships that could have appeared to influence the work reported in this paper.

Acknowledgements

None.

References

[1] Mok VCT, Cai Y, Markus HS. Vascular cognitive impairment and dementia: mechanisms, treatment, and future directions. Int J Stroke 2024;19(8):838. https://doi.org/10.1177/17474930241279888.
[2] Sweeney MD, Sagare AP, Zlokovic BV. Blood-brain barrier breakdown in Alzheimer disease and other neurodegenerative disorders. Nat Rev Neurol 2018;14(3):133–50. https://doi.org/10.1038/NRNEUROL.2017.188.
[3] Mortamais M, Artero S, Ritchie K. White matter hyperintensities as early and independent predictors of Alzheimer's Disease risk. Journal of Alzheimer's Disease 2014;42:S393–400. https://doi.org/10.3233/JAD-141473;WGROUP:STRING:PUBLICATION.
[4] Lee S, Viqar F, Zimmerman ME, et al. White matter hyperintensities are a core feature of Alzheimer's disease: evidence from the dominantly inherited Alzheimer network. Ann Neurol 2016;79(6):929. https://doi.org/10.1002/ANA.24647.
[5] Vipin A, Satish V, Saffari SE, et al. Dementia in Southeast Asia: influence of onset-type, education, and cerebrovascular disease. Alzheimers Res Ther 2021;13(1). https://doi.org/10.1186/S13195-021-00936-Y.

[6] Pantoni L. Cerebral small vessel disease: from pathogenesis and clinical characteristics to therapeutic challenges. Lancet Neurol 2010;9(7):689–701. https://doi.org/10.1016/S1474-4422(10)70104-6.

[7] Godin O, Maillard P, Crivello F, et al. Association of white-matter lesions with brain atrophy markers: the three-city Dijon MRI study. Cerebrovasc Dis 2009;28 (2):177–84. https://doi.org/10.1159/000226117.

[8] Vipin A, Loke YM, Liu S, et al. Cerebrovascular disease influences functional and structural network connectivity in patients with amnestic mild cognitive impairment and Alzheimer's disease. Alzheimers Res Ther 2018;10(1):82. https://doi.org/10.1186/s13195-018-0413-8.

[9] Rosenberg GA, Bjerke M, Wallin A. Multimodal markers of inflammation in the subcortical ischemic vascular disease type of vascular cognitive impairment. Stroke 2014;45(5):1531–8. https://doi.org/10.1161/STROKEAHA.113.004534/-/DC1.

[10] Zenaro E, Piacentino G, Constantin G. The blood-brain barrier in Alzheimer's disease. Neurobiol Dis 2017;107:41. https://doi.org/10.1016/J.NBD.2016.07.007.

[11] Li M, Li Y, Zuo L, Hu W, Jiang T. Increase of blood-brain barrier leakage is related to cognitive decline in vascular mild cognitive impairment. BMC Neurol 2021;21 (1):1–8. https://doi.org/10.1186/S12883-021-02189-6/TABLES/4.

[12] Bridges LR, Andoh J, Lawrence AJ, et al. Blood-brain barrier dysfunction and cerebral small vessel disease (Arteriolosclerosis) in brains of older people. J Neuropathol Exp Neurol 2014;73(11):1026. https://doi.org/10.1097/NEN.0000000000000124.

[13] Wang D, Chen F, Han Z, Yin Z, Ge X, Lei P. Relationship between amyloid-β deposition and blood–Brain barrier dysfunction in Alzheimer's disease. Front Cell Neurosci 2021;15. https://doi.org/10.3389/FNCEL.2021.695479.

[14] Huang J, Li J, Feng C, et al. Blood-brain barrier damage as the starting point of leukoaraiosis caused by cerebral chronic hypoperfusion and its involved mechanisms: effect of agrin and aquaporin-4. Biomed Res Int 2018;2018. https://doi.org/10.1155/2018/2321797.

[15] Rajeev V, Fann DY, Dinh QN, et al. Pathophysiology of blood brain barrier dysfunction during chronic cerebral hypoperfusion in vascular cognitive impairment. Theranostics 2022;12(4):1639. https://doi.org/10.7150/THNO.68304.

[16] Montagne A, Barnes SR, Sweeney MD, et al. Blood-brain barrier breakdown in the aging human hippocampus. Neuron 2015;85(2):296–302. https://doi.org/10.1016/J.NEURON.2014.12.032.

[17] Nitta T, Hata M, Gotoh S, et al. Size-selective loosening of the blood-brain barrier in claudin-5-deficient mice. J Cell Biol 2003;161(3):653–60. https://doi.org/10.1083/JCB.200302070.

[18] Zhang CE, Wong SM, Van De Haar HJ, et al. Blood-brain barrier leakage is more widespread in patients with cerebral small vessel disease. Neurology 2017;88(5): 426–32. https://doi.org/10.1212/WNL.0000000000003556/SUPPL_FILE/ZHANG_426.PDF.

[19] Shao X, Jann K, Ma SJ, et al. Comparison between blood-brain barrier water exchange rate and permeability to gadolinium-based contrast agent in an elderly cohort. Front Neurosci 2020;14. https://doi.org/10.3389/FNINS.2020.571480.

[20] Mahroo A, Konstandin S, Günther M. Blood–Brain barrier permeability to water measured using multiple echo time arterial spin labeling MRI in the aging Human brain. Journal of Magnetic Resonance Imaging 2023;59(4):1269–82. https://doi.org/10.1002/JMRI.28874.

[21] Padrela B, Mahroo A, Tee M, et al. Protocol: developing blood-brain barrier arterial spin labelling as a non-invasive early biomarker of Alzheimer's disease (DEBBIE-AD): a prospective observational multicohort study protocol. BMJ Open 2024;14 (3). https://doi.org/10.1136/BMJOPEN-2023-081635.

[22] Lin Z, Jiang D, Liu D, et al. Noncontrast assessment of blood-brain barrier permeability to water: shorter acquisition, test-retest reproducibility, and comparison with contrast-based method. Magn Reson Med 2021;86(1):143–56. https://doi.org/10.1002/MRM.28687.

[23] Leow YJ, Wang JDJ, Vipin A, et al. Biomarkers and cognition study, Singapore (BIOCIS): protocol, study design, and preliminary findings. J Prev Alzheimers Dis. 2024:1–13. https://doi.org/10.14283/JPAD.2024.89/TABLES/3. Published online May 21.

[24] Günther M, Oshio K, Feinberg DA. Single-shot 3D imaging techniques improve arterial spin labeling perfusion measurements. Magn Reson Med 2005;54(2): 491–8. https://doi.org/10.1002/MRM.20580.

[25] von Samson-Himmelstjerna F, Madai VI, Sobesky J, Guenther M. Walsh-ordered hadamard time-encoded pseudocontinuous ASL (WH pCASL). Magn Reson Med 2016;76(6):1814–24. https://doi.org/10.1002/MRM.26078.

[26] Schmidt P, Gaser C, Arsic M, et al. An automated tool for detection of FLAIR-hyperintense white-matter lesions in Multiple Sclerosis. Neuroimage 2012;59(4): 3774–83. https://doi.org/10.1016/j.neuroimage.2011.11.032.

[27] Hu LT, Bentler PM. Cutoff criteria for fit indexes in covariance structure analysis: conventional criteria versus new alternatives. Struct Equ Modeling 1999;6(1): 1–55. https://doi.org/10.1080/10705519909540118.

[28] Stewart CR, Stringer MS, Shi Y, Thrippleton MJ, Wardlaw JM. Associations between white matter hyperintensity burden, cerebral blood flow and transit time in small vessel disease: an updated meta-analysis. Front Neurol 2021;12:647848. https://doi.org/10.3389/FNEUR.2021.647848/FULL.

[29] Staffaroni AM, Cobigo Y, Elahi FM, et al. A longitudinal characterization of perfusion in the aging brain and associations with cognition and neural structure. Hum Brain Mapp 2019;40(12):3522–33. https://doi.org/10.1002/HBM.24613.

[30] Zhang R, Huang P, Wang S, et al. Decreased cerebral blood flow and delayed arterial transit are independently associated with white matter hyperintensity. Front Aging Neurosci 2022;14. https://doi.org/10.3389/FNAGI.2022.762745/FULL.

[31] Fernando MS, Simpson JE, Matthews F, et al. White matter lesions in an unselected cohort of the elderly: molecular pathology suggests origin from chronic hypoperfusion injury. Stroke 2006;37(6):1391–8. https://doi.org/10.1161/01.STR.0000221308.94473.14.

[32] Seo JH, Miyamoto N, Hayakawa K, et al. Oligodendrocyte precursors induce early blood-brain barrier opening after white matter injury. J Clin Invest 2013;123(2): 782. https://doi.org/10.1172/JCI65863.

[33] Persyn E, Hanscombe KB, Howson JMM, Lewis CM, Traylor M, Markus HS. Genome-wide association study of MRI markers of cerebral small vessel disease in 42,310 participants. Nat Commun 2020;11(1). https://doi.org/10.1038/S41467-020-15932-3.

[34] Koohi F, Harshfield EL, HS Markus. Contribution of conventional cardiovascular risk factors to brain white matter hyperintensities. J Am Heart Assoc 2023;12(14): 30676. https://doi.org/10.1161/JAHA.123.030676/ASSET/2AF0B198-32A9-4C50-8F35-5D30BE75A97E/ASSETS/GRAPHIC/JAH38631-FIG-0003.PNG.

[35] Wardlaw JM, Sandercock PAG, Dennis MS, Starr J. Is breakdown of the blood-brain barrier responsible for lacunar stroke, leukoaraiosis, and dementia? Stroke 2003;34 (3):806–11. https://doi.org/10.1161/01.STR.0000058480.77236.B3.

[36] Sam K, Peltenburg B, Conklin J, et al. Cerebrovascular reactivity and white matter integrity. Neurology 2016;87(22):2333. https://doi.org/10.1212/WNL.0000000000003373.

[37] Starr JM, Wardlaw JM, Ferguson K, MacLullich A, Deary IJ, Marshall I. Increased blood-brain barrier permeability in type II diabetes demonstrated by gadolinium magnetic resonance imaging. J Neurol Neurosurg Psychiatry 2003;74(1):70–6. https://doi.org/10.1136/JNNP.74.1.70.

[38] Takechi R, Lam V, Brook E, et al. Blood-brain barrier dysfunction precedes cognitive decline and neurodegeneration in diabetic insulin resistant mouse model: an implication for causal link. Front Aging Neurosci 2017;9(DEC):316877. https://doi.org/10.3389/FNAGI.2017.00399/BIBTEX.

[39] Chau ACM, Cheung EYW, Chan KH, et al. Impaired cerebral blood flow in type 2 diabetes mellitus – A comparative study with subjective cognitive decline, vascular dementia and Alzheimer's disease subjects. Neuroimage Clin 2020;27:102302. https://doi.org/10.1016/J.NICL.2020.102302.

[40] Hainsworth AH, Markus HS, Schneider JA. Cerebral small vessel disease, hypertension, and vascular contributions to cognitive impairment and dementia. Hypertension 2023;81(1):75. https://doi.org/10.1161/HYPERTENSIONAHA.123.19943.

[41] Biesbroek JM, De Kort FAS, Anblagan D, et al. Signature white matter hyperintensity locations associated with vascular risk factors derived from 15 653 individuals. Stroke 2025;56:3047–59. https://doi.org/10.1161/STROKEAHA.125.051159;ISSUE:ISSUE:DOI.

[42] Wardlaw JM, Valdés Hernández MC, Muñoz-Maniega S. What are white matter hyperintensities made of? Relevance to vascular cognitive impairment. J Am Heart Assoc 2015;4(6):001140. https://doi.org/10.1161/JAHA.114.001140.

[43] Blevins BL, Vinters HV, Love S, et al. Brain arteriolosclerosis. Acta Neuropathol 2021;141(1). https://doi.org/10.1007/S00401-020-02235-6.

[44] Farhoudi M, Mehrvar K, Aslanabadi N, Ghabili K, Rasi Baghmishe N, Ilkhchoei F. Doppler study of cerebral arteries in hypercholesterolemia. Vasc Health Risk Manag 2011;7(1):203. https://doi.org/10.2147/VHRM.S18663.